Lab on a Chip

Accepted Manuscript

ROYAL SOCIETY OF CHEMISTRY

www.rsc.org/loc

Lab on a Chip

ARTICLE

Centrifugal microfluidic platform for single-cell level cardiomyocyte-based drug profiling and screening

Received 00th January 20xx,
Accepted 00th January 20xx

DOI: 10.1039/x0xx00000x

www.rsc.org/

W. Espulgar,[a*] W. Aoki,[a] T. Ikeuchi,[a] D. Mita,[a] M. Saito,[a] J.-K. Lee,[b] E. Tamiya[a*]

Drug screening and profiling is an important phase in drug discovery, development, and marketing. However, some profiling tests are not routinely done because of the needed additional technical skill and costly maintenance, which leads to cases of unexpected side effects or adverse drug reactions (ADRs). This study presents the design and operation of a microfluidic chip for single-cell level drug screening and profiling as an alternative platform for this purpose. Centrifugation was utilized to trap isolated single and groups of primary culture neonatal rat cardiomyocytes in the same chip. In the off-spin operation of the chip, the cells can be observed under a microscope and movies of the beat motion can be recorded. Beat profiles of the cells were generated using image correlation analysis of the recorded video to study the contractile characteristics (beating rate, beating strength, and inter-beat duration). By utilizing this non-invasive tool, long term continuous monitoring, right after trapping, was made possible and cell growth and dynamics were successfully observed in the chip. Media and liquid replacement does not require further centrifugation but instead utilize capillary flow only. The effect of carbachol (100 μM) and isoproterenol (4 μg/mL) to single cells and groups of cells were demonstrated and the feature for immunostaining (β-actin) applicability of the chip was revealed. Furthermore, these findings can be helpful for the headway of non-invasive profiling of cardiomyocytes and for future chip design and operation of high-throughput lab on-a-chip devices.

Introduction

Profiling of chemical entities is essential in early phases of drug discovery and development.[1] In the past years, there has been a great increase in research and development of the pharmaceutical industry[2] but only a meagre 11% of these compounds were successfully developed and registered in 1991-2000 from the ten big pharma companies in the United States and in Europe.[3] About 30% of these failures were associated to toxicity and safety issues.[1] In addition, even after successful registration, the drug can be withdrawn from the market because of unintended and undesired responses that is beyond their anticipated therapeutic effect during the clinical use at normal dose. It is estimated that 6–7% of hospitalized patients experience this severe adverse drug reactions (ADRs) each year with a potential of 100,000 deaths making it the fourth largest cause of death in the USA.[4] Anticipating this likely side effect profile of drugs is therefore with utmost importance in the present drug discovery, development, and marketing.

A review of drug attrition in non-clinical and clinical development reports revealed that cardiovascular toxicity occurred more frequently than hepatoxicity.[5] Cardiovascular events emerged when drugs were administered for longer period of times to larger patient population.[5] In 1990–2006, one-third of all drug withdrawals in the US were associated to drug-induced Torsades de Pointes, a potentially fatal arrhythmia.[5] There are existing sensitive and predictive imaging technologies to measure changes in cardiac electrophysiological function to address this problem; however, they are not routinely available in all laboratories and therefore not consistently included in drug development programs[5] for it requires additional technical skill and discipline and costly maintenance.

And thus, the purpose of this study is to develop a centrifugal microfluidic chip as a cheap and easy platform for cardiomyocyte-based drug screening and profiling purposes in single cell level. Single cell analysis has unique phenomena that are usually masked by the average response from a cell population; therefore, studying the effects to individual cells can provide new insights for drug profiling. Most pharmaceutical companies are familiar with cell-based safety screen for rapidly screening the compounds during initial discovery phase and for mechanistic and detailed studies during the developmental phase.[2] The use of cell-based technology for drug discovery provides interrogation of targets and pathways in a more physiological setting compared to biochemical assay.[6] In addition, signalling pathways within the cell and cellular processes (proliferation, migration, adhesion,

[a] Department of Applied Physics, Graduate School of Engineering, Osaka University, 2-1 Yamadaoka, Suita, Osaka 565-0871, Japan. E-mail: wilfred@ap.eng.osaka-u.ac.jp, tamiya@ap.eng.osaka-u.ac.jp
[b] Department of Cardiovascular Regenerative Medicine, Graduate School of Medicine, Osaka University, 2-2 Yamadaoka, Suita, Osaka 565-0871, Japan.
†Electronic Supplementary Information (ESI) available: See
DOI: 10.1039/x0xx00000x

and apoptosis) could be associated with very specific and well-defined changes in cell morphology and adhesion.[6] Monitoring these changes can provide insights on *in vivo* pathophysiology in the cells and help the advancement of drug development.

The use of centrifugal microfluidics has been utilized in a range of applications.[7–12] Aside from providing precise spatio-temporal control of medium conditions, parallelization, cell confinement,[13] and relatively cheap method of microfluidics, centrifugation is a common practice in general chemical and biological laboratory. Thus, operation to conduct experiments on cells using the microfluidic chip will pose minimal problem even for those who are not familiar with microfluidics technology.

In a rotating chamber, the centrifugal force, F_c, applied is:[7]

$$F_c = \frac{\pi}{6} {D_p}^3 (\rho_p - \rho_f) r \omega^2, \quad (1)$$

where D_p is the particle diameter, ρ_p and ρ_f are the densities of the particle and the fluid, respectively, *r* is the particle position from the center of rotation, and ω is the angular velocity of rotation. This is opposed by the drag force, F_d, on a particle following the equation when *Re* is sufficiently small (*Re*<1):

$$F_d = 3\pi\eta D_p U_{(r)}, \quad (2)$$

where η is the fluid viscosity and $U_{(r)}$ is the average flow velocity at a point r from the center.[7] Provided that the cells are uniform and no change in the suspension fluid, the centrifugal force can easily offset the drag force and scaled by simply increasing the rotation speed and in effect produce fluid flow through the channels. In addition, fluid flow induced by centrifugation has a constant flow rate.[14] This makes it a good alternative for large syringe pumps that are used in common microfluidic devices. This method was utilized to manipulate the cells in the device and be captured on the trap sites due to sedimentation; another unique feature of centrifugal microfluidics.

Particle manipulation and trapping by centrifugation was first reported by Burger et al.[15,16] This demonstrated the sedimentation effect to trap particles in an array of mechanical traps. The number of trapped particles can be influenced by the particle diameter and the capture area. An array of traps has also been reported to capture and monitor single HeLa cells in a pump-driven microfluidic chip.[17]

In this microfluidic chip, cells can be observed right after trapping and be monitored after in real-time under a microscope. Single cell and cells in a group could be studied in the same device with few microliters of liquid. Media replacement in the chip was done by exploiting capillary flow controlled by simply aspirating the excess liquid from the outlet. Since trap sites were predetermined, location and monitoring of the cells were made easy. This is beneficial in immunostaining; a common and indispensable biological laboratory practice. This is more advantageous than using the conventional petri dish-based assay where locating and monitoring cells can be a painstaking task.

Image correlation analysis or motion vector analysis was also utilized in analysing the video images of beating neonatal rat cardiomyocytes and evaluate the contractile characteristics. Label-free video microscopy is advantageous since it's non-invasive and therefore live cells present can be monitored continuously. This method calculates the velocity field over the selected image that can generate parameters such as the average contractile speed, global deformation, and contraction propagation.[18–20] These could be combined with the beat rate and beat profile analyses to make a sound judgment on the condition of the cell. In addition, such parameters can be associated to the ion channels conditions, beat strength, and beat direction of the cell and demonstrated to be useful in drug screening studies.[18]

Optimizing the use of video analysis method to study the trapped cells in the centrifugal microfluidic chip, it is believed that this tool can greatly help the pharmaceutical industry for pharmacological profiling of the cardiovascular effect in drug development. This report, however, primarily focuses on the device fabrication and operation to disclose the features of the device and its applicability and limitation for drug screening and related studies.

Materials and methods

Mold design

Fig. 1a shows the features of the mold design which resembles that of a sakura flower (cherry blossom). The design has 5 trap areas where each area has its own unique trap design. Three of the trap areas were intended for single cell trapping while the remaining two were intended for multiple cell trapping. From the central inlet, cell suspension will flow radially outward to enter the trap area. One trap area has four channels that contain the trap sites (Fig. 1b–1d). To ensure that the top layer of the channel will not sag or collapse, cylindrical posts were included in the design at the entry of the channels which can be helpful in filtering the cell suspension (Fig. 1b). The gap size of the trap sites were set to 8 μm to capture the neonatal rat cardiomyocyte cells with observed size ranges from 12–15 μm. Hydrodynamic trapping, which is widely used in microfluidics,[21] was utilized in this design in addition to the sedimentation effect of centrifugation. Untrapped cells and excess fluid will exit at the outlet of the trap area after passage.

Mold fabrication and chip assembly

The mold and the chip were fabricated similar to the technique in the previous report.[22] Briefly, a 36 μm thick SU-8 3025 (Microchem, Newton, MA, USA) photoresist was developed in pattern with the mold design on a clean silicon wafer. A 1 mm thick acrylic plastic, shaped accordingly to the central area, was then bonded at the center of the developed photoresist using a double-sided tape (Fig. 1f). This provided the space that served as fluid reservoir for each trap area. For the central inlet mold, the base of a metal cylinder with 5 mm diameter and 12 mm height was glued at the center of the acrylic plastic. For the outlet mold, metal rivets with 1 mm diameter and 5 mm height cylindrical shaft and with 3 mm diameter head were used. The head part was glued to the developed photoresist. Upon completion of the master mold, silicon

tubes were inserted to the metal post and rivets (Fig. 1g). For the inlet, a silicon tube with 5 mm inner diameter and 6 mm outer diameter and 15mm height was used. For the outlet, a silicon tube with 1 mm inner diameter and 3 mm outer diameter and 13 mm height was used. A 10-to-1 mixture of PDMS monomer and initiator agent (Dow Corning, Midland, MI, USA) was casted on the mold afterwards. The casted PDMS on the mold was baked at 80 ˚C for 1 h for polymerization. Lower temperature (60 ˚C for 5 h) was utilized when the mold was used for the first time to avoid the adhesive from melting. A cured PDMS microfluidic network was then demolded, cut into appropriate dimension, and plasma bonded to a 0.17 mm thick clean glass slide (5 cm x 7 cm dimension) (Fig. 1h). The assembled chip was heated afterwards at 65 ˚C for 30 min to let the surfaces bond firmly.

Chip usage protocol

Pre-cell handling treatment of the chip and cell suspension preparation were based on the previous report.[22] Cell concentration of 1 x10^5/mL of primary cultures of neonatal rat cardiomyocytes was prepared in this study. Cells were supplied by the Graduate School of Medicine, Osaka University and all procedures performed to harvest the cells are in compliance with the guidelines set by the Animal Experiments Committee of Osaka University. Three hundred fifty (350) microliters of the cell suspension was poured into the chip inlet. The chip was then carefully placed on a spin coater (MS-A100, Mikasa, Tokyo, Japan) and the assembly was spun at 500 rpm for 30 s and then raised and maintained at 1500 rpm for 3 min where 100 rpm/s was set as the rate for acceleration and deceleration; 4 min operation in total. After centrifugation, the chip was placed inside a petri dish to avoid contamination and the culture media was then refilled into the inlet. The trapped cells can be checked right after trapping using an inverted microscope (IX 71 Inverted Microscope, Olympus, Tokyo, Japan) with stage heated at 37 ˚C. Continuous monitoring can also be done readily or the chip can be maintained at 37 ˚C in a humidified incubator with 5% CO_2 for desired time span. The residence time for the culture media replacement is 24 h. The old culture media at the inlet was aspirated while that at the outlet was sip out by a syringe. The fresh culture media was poured into the inlet where media replacement utilized capillary flow (1.4 µL/min) only without the need for external interconnects.

Video analysis

The spontaneous beatings of the cardiomyocytes were recorded using a high speed camera (HAS-L2, DITECT, Tokyo, Japan) mounted on the inverted microscope for 1–2 min with stage heated at 37 ˚C. Frame rate of 30–150 fps were used with 680 x 512 resolution viewed under a x20 or x40 objective lense. Motion vectors of the beating cardiomyocytes were

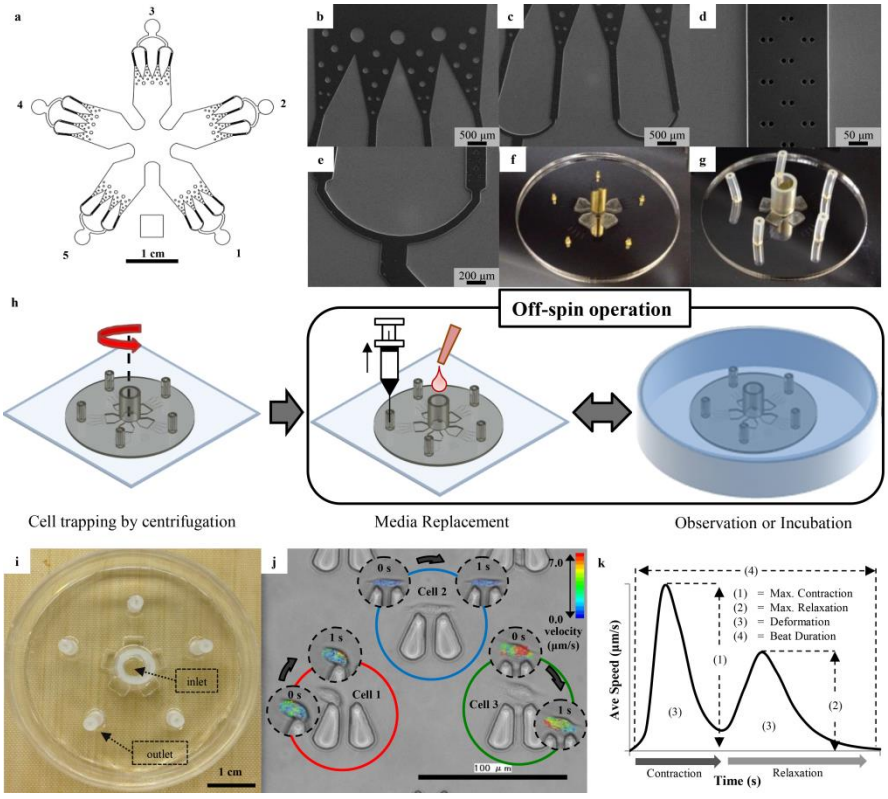

Fig. 1. Trap design, chip operation, and beat profile generation. (a) 2D Wireframe design showing 5 trap areas. (b) Filtering area where columns served as sieves that filter out unwanted particles. The trap channels (c–d) in one trap area converges into one (e) outlet. The chip was fabricated using a (f) master mold where (g) silicon tubes were inserted into metal cylinders that served as inlet and outlets. (h) The chip is rotated to trap cardiomyocytes. Observation, media replacement, video recording, and drug screening were done during off-spin operation. (i) Cured chip on glass substrate. (j) Generated beat motion image of observed single cells. Cell 2 is not beating. (j) Notation used from the generated graph where maximum contraction, relaxation deformation and beat duration are derived in addition to beat rate.

obtained using block matching algorithm[18] utilized in Flownizer (DITECT, Tokyo, Japan). In this study, a 5 µm x 5 µm integration block was used for the algorithm. By getting the average speed of the blocks covering the 2D surface area of the cell (Fig. 1j), the beat profile was generated which reflects its electrophysiological condition. Analysis of the generated graph was done with the aid of Peakfit (Systat Software Inc., CA, USA). Fig. 1k illustrates the single beat representation of a cardiomyocyte cell which was analyzed based on a reported approach[18] and served as the basis for comparison among observed cells. One beat corresponds to two peaks which are the contraction and relaxation motion. Deformation, which is related to the beat strength, or the total area under the curve and beat duration can also be quantified in addition to beat rate for analyzing the cell. Actual quantification of contractile force was not done in this study. Provided that no change in the substrate's modulus of elasticity, relative comparison of beat strength can be done by simply comparing the areas under the curves of interest.

Drug application test

After culturing the cells for 3 days, administration of drugs was conducted. Concentration of 100 µM of carbachol (Sigma-Aldrich, St. Louis, MO, USA) and 4 µg/mL of isoproterenol (Kowa group, Nagoya, Japan) diluted in warm culture media were prepared. Three hundred and fifty (350) microliters from each solution was poured into the inlet of separate chips after aspirating the old culture media and were then placed inside a humidified incubator with 5% CO_2 at 37 ˚C. Prior to drug administration, cells were observed and videos were recorded. After 10 min, the same cells were observed, videos were recorded and beat profiles were then compared. Video recording was done based on the video analysis section.

Beta actin immunostaining

All liquid passage and replacement in the chip were done using centrifugation again. The same setting used in cell trapping was set except for the maximum rotation speed which was reduced to 1000 rpm for 1 min; 2 min operation in total. Samples were washed with phosphate buffered saline (PBS) after removing supernatant and culture media and the cells were fixed with 4% PFA (Paraformaldehyde) for 15 min at room temperature. The channels were then washed with PBS before adding 100 µL of 0.2% Triton X-100 diluted in PBS for permeabilization and incubated for 15 min at room temperature. After washing with PBS, 100 µL of 1% BSA in PBS for blocking was added and incubated for 60 min at room temperature. The cells were then exposed to 100 µL of Rabbit Anti-beta Actin Polyclonal Antibody, Cy3 conjugated (Bioss Inc., Woburn, MA, USA) solution (1:100 dilution in 1% BSA-PBS) and incubated for 60 min at 4 °C. Without washing, DAPI (VECTASHIELD Antifade Mounting Medium with DAPI, Vector Laboratories Inc., Burlingame, CA, USA) solution was added and the chip was observed under a confocal microscope (A1 MP, Nikon, Tokyo, Japan).

To serve as standard and basis for comparison, 10^5 of the cells from the same cell suspension were resuspended in 2 mL of the same culture media and were then plated in a 32-mm gelatin-coated petri dish. Cells grown on the petri dish were observed and tested consecutively with the cells grown on the microfluidic chip and the beating behaviors were analyzed using the same imaging analysis algorithm.

Results and discussions

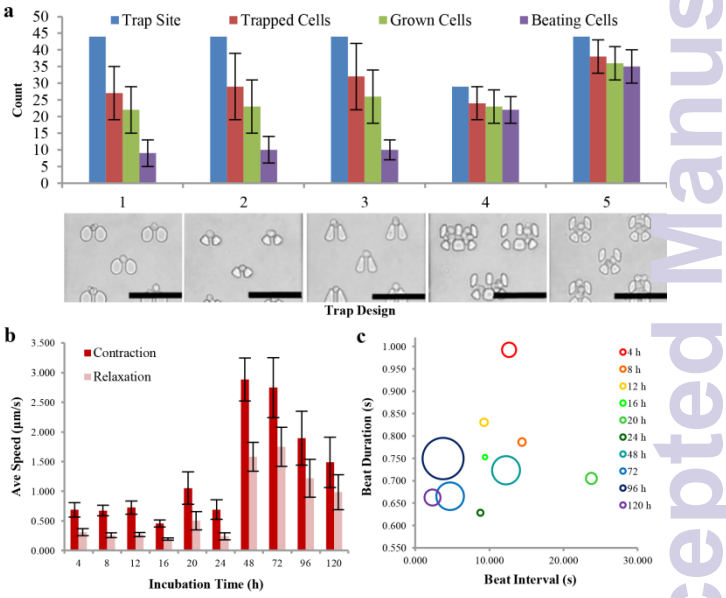

Fig. 2. Trapping capability of the designed chip and growth of isolated single cells. (a) Cardiomyocytes trapped at different areas: 1–3 for single cell trapping and 4–5 for multiple cell trapping (Scale bar, 100 µm). Images are obtained right after trapping. Counting for trapped cells in traps 4–5 is only based on if the cells are trapped or not and not the total number of cells pe each site. Number of trapped cells that exhibit growth and beating was also counted. 70–80% of the trapped cells grew and 30% exhibited beating for single cell trapping. Error bars represent standard deviation of the mean (n= 40; 4 trap channels of each trap area for 10 trials observing ~1000 cells). A higher percentage of the cells grew and exhibited beating in the multiple ce trap. (b) Comparison of maximum cell contraction and relaxation. Error bars represent standard error of the mean (n=50). (c) Depiction of beat interva beat duration, and beat strength (area of the circle) of the observed cells for 5 days.

Cell trapping and growth monitoring

Trapping the cells in the desired location is one of the key features of the designed chip. Fig. 2a presents the trapping capability of the designed chip based on 10 trials using 3 batches of cardiomyocyte suspension. The chip has 5 trap areas where trap areas 1–3 were intended for single cell trapping while trap areas 4–5 were intended for multiple cell trapping. The location of the sites (100 µm center-to-center distance) designed for single cell trapping were set such that interaction between cells can be avoided and thus isolated cells can be observed. The separation distance set was based from the findings in a previous report.[22] The design for the multiple cell trapping was made for easy passage of the culture media while the cells are trapped. A multiple cell trap site had the ability to capture 2–10 cells. Based from the graph, the

trapping capability of the single traps (60%–70%) is lower than the multiple cell traps (90%). This is expected since the distance between trap sites for single cell trapping is maximized and thus existence of stream lines that do not interact with the trap sites is high; some of the cells can avoid the trap sites. The number of cells that grew and exhibited beat was also counted. For single cell traps, 70–80% of the trapped cells grew and 30% exhibited beating after one day of incubation. The design structure of the trap site for single cell trapping was found to have no significant effect to the growth of the cell and to the trapping capability of the chip. A higher percentage of the cells grew and exhibited beating in the multiple cell traps and had the same viability (80%) with the cells grown in a petri dish. A cardiomyocyte cell usually requires an external stimulus for it to beat; and thus, a higher chance of beating is expected for cells in a group. Still, single cell beating is possible since neonatal cardiomyocyte cells were used in this study. Based on observation, some cells are already beating right after trapping in the chip. This device provided the capability to identify readily and isolate individual cells for easy observation.

For future studies, it is important to know the growth condition of the cells and the corresponding time of occurrence. This can be helpful in designing future studies depending on the target phenomenon. The device provided the capability of monitoring the cells even right after trapping. This is advantageous compared to the conventional petri dish approach where cells need to settle down first and grow at the bottom of the dish. Fig. 2b–2c presents the analysis done on 50 single cells that were observed for 5 days. Parameters were derived from the image correlation analysis discussed in the method section. A summary of the generated values is made available in Supplementary Table 1. Based on the graphs, the maximum contraction and relaxation were observed at day 2 and the maximum beat strength and stable beat rate were observed at 3–5 days. Thus, for single cell observation, the optimum status of the cell is decided to be after 3–4 days of incubation. The number of beating single cells abruptly decreased after 5 days. It is believed that most of the trapped isolated single cardiomyocytes undergo deterioration that leads to cell death after 5 days of incubation. However, monitoring cell death and the stages undergone are not covered in this report.

Fig. 3 shows the continuous monitoring of a group of observed cells. Group of cells trapped in the chip can last for two weeks. Cell spreading was observed at 20 h after incubation (Fig. 3e). Cell 2 and cell 4, that exhibited beating as early as 4 h, were observed to be the ones that migrate and spread the most. Cell 1 and cell 2 that were in contact demonstrated harmonious beating after 4 days of incubation (Fig. 3i, Movie 1) and a succession of beating can be noticed based on the beat profiles (Fig. 3k) indicating that the cells were connected physically and electrically. The cells undergone coupling and decoupling connection throughout the duration of observation which is similar to the previous report[22] but observed to stabilize after 4 days of incubation. Fig. 3j shows the beat rate variation (18 bpm at max) of the observed cells depicting couple shifting throughout the duration of the observation. This phenomena is not yet fully understood but is associated to the cell heterogeneity and beat rate matching. Based on these observations, it is inevitable to note that a direct physical contact between cells does not assure a successful connection and beating between cells. This can be useful for studying drug-induced cell connection and disconnection which will not be disclosed in this report. Identifying how neonatal cardiomyocytes form gap junctions or intercellular connections and the determining factors for optimum connection are still ambiguous in the current framework.

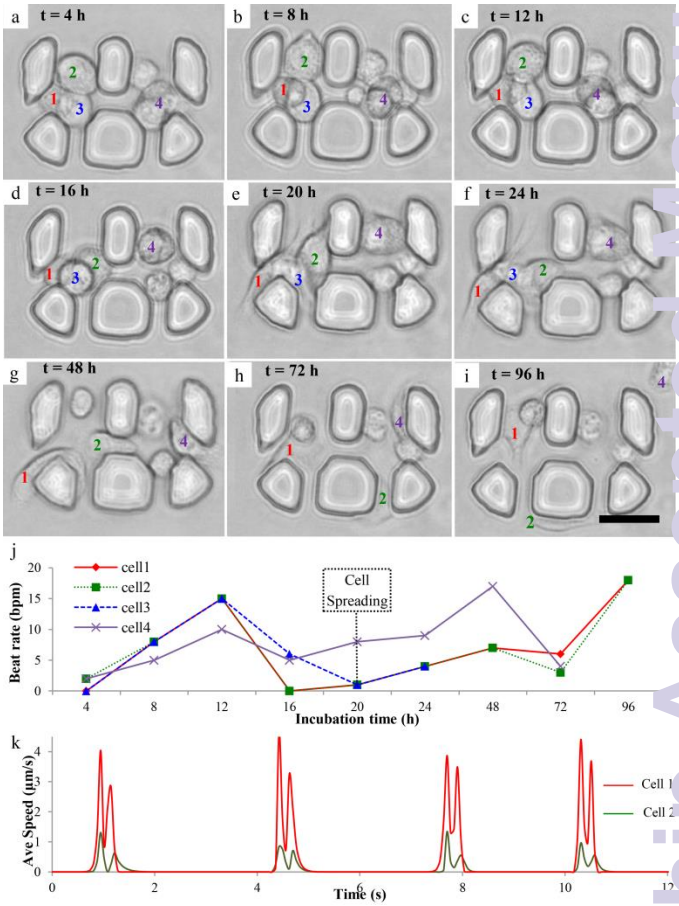

Fig. 3. Monitored group of cells. (a–i) Cells were observed every 4 h. (j) Beat rate variation of monitored cells. (k) Beat profiles of cell 1 and cell 2 after 4 days. (Scale bar, 25 μm)

Comparison of single cardiomyocytes and group of cardiomyocytes trapped in the chip

Cells were observed after 4 days of incubation for optimum coupling of cells in a group. Fig. 4 presents the motion vector and beat profile of a single cardiomyocyte (Fig. 4a–4d, Movie 2) and a group with ~ 4 cells (Fig. 4e–4h, Movie 3). Expectedly, cells in a group have a more stable beating than a single cell; higher beat rate, contraction speed, relaxation speed, and deformation were observed in a group of cells. However, it is interesting to note that, based on observation, the shape of the generated graph for a single cell can vary from one cell to another. Ventricular and atrial cardiomyocytes are the known

working types of cardiomyocytes. Ventricular cardiomyocytes display homogenous contraction-relaxation response throughout the cell while, in contrast, atrial cardiomyocytes display initiation contraction-relaxation response around the periphery of the cell.[23] These can be reflected on the shape of the generated graph and can be tapped as a way to categorize the type of cells present and be an extension for future study.

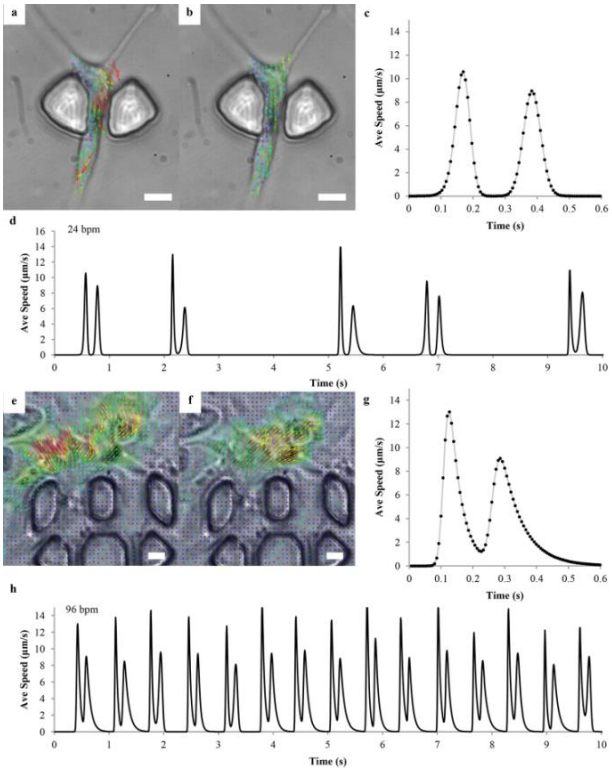

Fig. 4. Beat profile comparison. Single cell: (a) contraction, (b) relaxation, (c) single beat, and (d) beat profile. Group of cells: (e) contraction, (f) relaxation, (g) single beat, and (h) beat profile. Color and length of the arrow represent the magnitude of the motion and direction of the arrow represents the direction of motion of the 5 μm x 5 μm block. Motion vectors outside the cell is also shown but not included in the beat profile generation. (Scale bar, 10 μm)

To determine the condition of the cytoskeleton of the trapped cells and ensure that single cells are isolated, β-actin immunostaining was done. Fig. 5 contains the images of the stained cells. It can be observed from Fig. 5b that a single rod-shaped cell has β-actin distribution concentrated along the edges. This is verified by the 3D image (Fig. 5c) generated from the same cell. Comparing the direction of contraction-relaxation of the cell (Fig. 5d–5e), it can be seen that it coincides with the β-actin distribution. The concentration and arrangement of β-actin can therefore be correlated to the cells' contractility. The more organized the distribution is, the more contractile the cell is.[23,24] Fig. 5f shows the comparison of a beating single cell and a group of beating cells. A striated distribution of β-actin can be observed in the single cell. However, no pattern was seen in a group of cells. High contractility was observed in the group of cells but the direction of motion does not coincide with the β-actin distribution. A possible reason for this is the presence of a pacemaker cell in the group. Pacemaker cells are non-beating cardiomyocytes that fire signal to and drive beating from the cells surrounding it.[25,26] However, identifying which among the cells is the pacemaker type is a current limitation of the device and the method. Also, another target (e.g. actinin or myosin) for immunostaining may be needed. More importantly, immunostaining was successfully done in the chip which can be helpful for cell study and other related matters.

In comparison to an adult cardiomyocyte with adherens and gap junctions present at intercalated disc of individual cells and intact T-tubules, neonatal cardiomyocytes form adherens and gap junctions dynamically with neighboring cell and have no T-tubules.[27] In addition, neonatal rat cardiomyocytes can coexpress more than one connexin or gap junction protein isoform which are able to form homometric-homotypic gap junction channels aside from potential homometric-heterotypic, heterometric-homotypic, and heterometri-heterotypic channels.[28] The gating behavior of the channels is affected by the length and type of the connexin present and, in effect, signal transmission between cells can be obstructed. And thus, asymmetric behavior observed in a group of cells is due to the voltage sensitivity difference between cardiomyocytes.

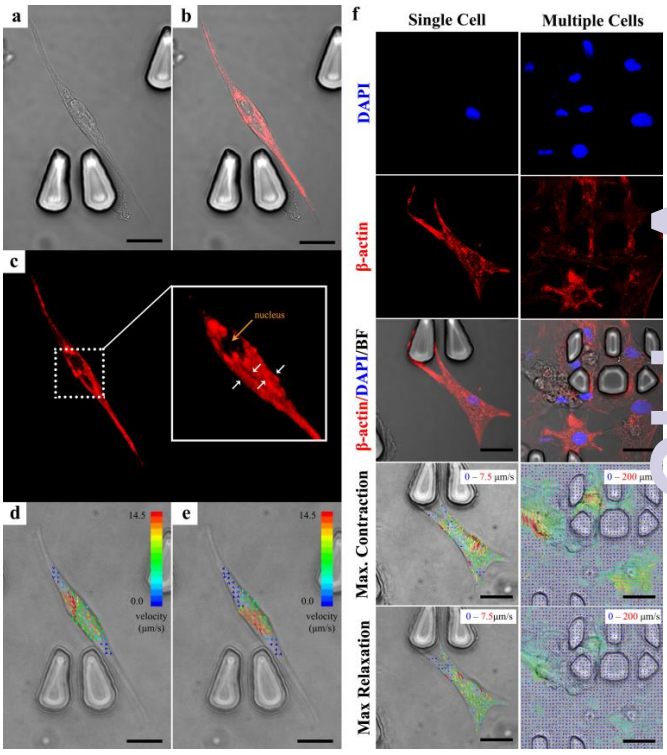

Fig. 5. β-actin immunostaining and beat motion. (a) Bright field (BF) image (b) BF and β-actin staining and (c) distribution of β-actin in 2D and 3D view in a single cell. (d) Maximum contraction. (e) Maximum relaxation. Arrows represent the direction of motion where color and length depicts the magnitude. (f) Comparison of a single cell and a group of cells after 4 days of incubation in the same chip. All possible motion is shown in a group of cells but only motion vectors covering the cells are used for analysis. (Scale bar, 25 μm)

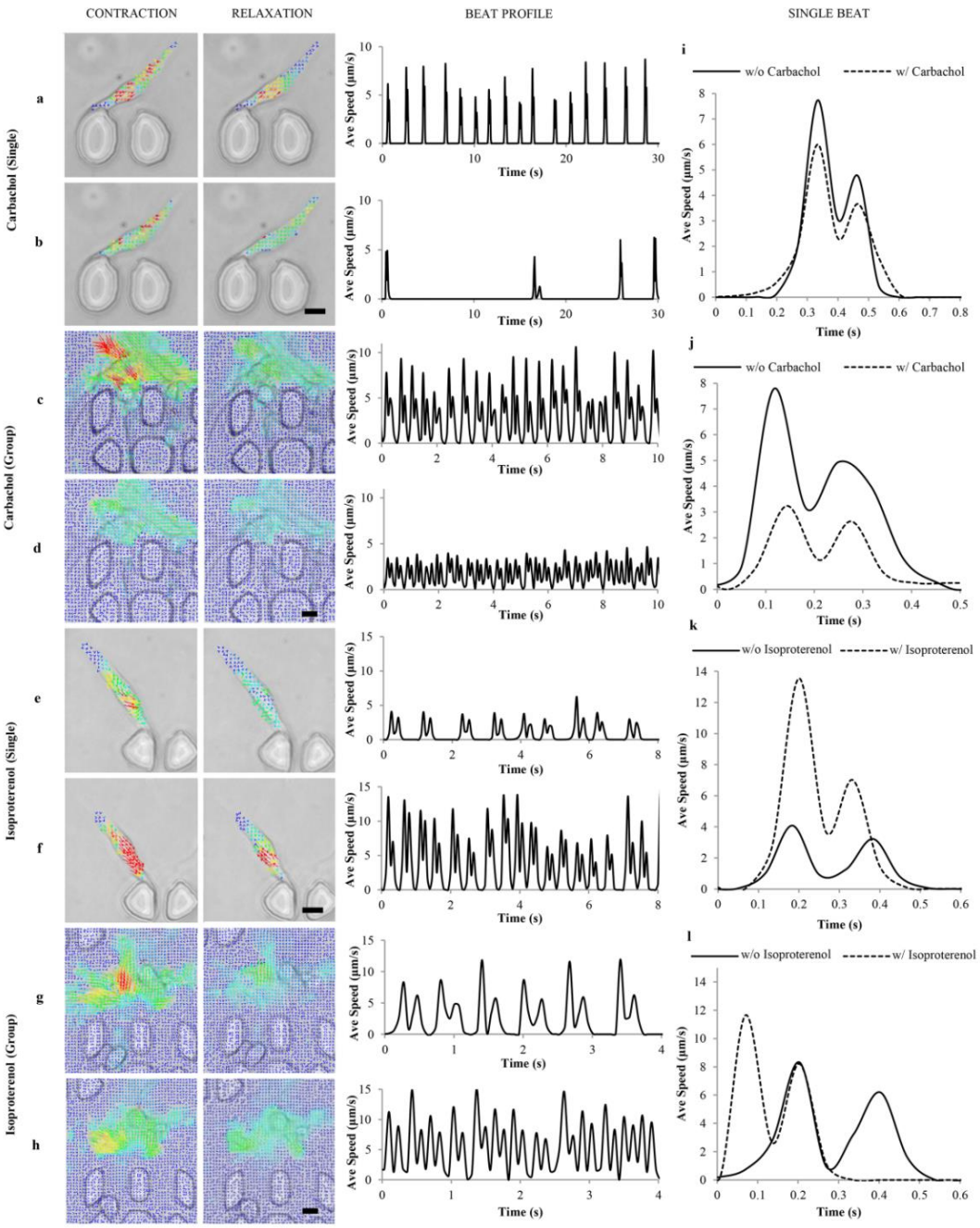

Fig. 6. Beat motions and beat profiles before (a,c,e,g) and after (b,d,f,h) administration of drugs in separated chips. 100 μM of carbachol exposed to a single cell (a–b) and a group of cell (c–d) and the corresponding single beat profiles (i–j). 4 μg/mL of isoproterenol exposed to a single cell (e–f) and a group of cell (g–h) and the corresponding single beat profiles (k–l). (Scale bar, 20 μm).

Drug effect trial

Carbachol is commonly used for a range of ophthalmic purposes and is a muscarinic agonist.[29] It activates the muscarinic acetylcholine receptor, which in effect, lowers the beat rate of the cell. Fig. 6a–6d contains the effect to a single cell (Movie 4) and a group of cells (Movie 6) after 10 min of exposure to carbachol (Movie 5 for single cell and Movie 7 for group of cells). The single cell had a 94% decrease in beat rate and 50% increase in beat duration. The beat strength of the cell did not change since the area under the curve remained constant. For a group of cell, the beat strength decreased by 50% and beat duration decreased by 15% but had 2.5x increase in beat rate. The effect of carbachol to different groups of cells had varying results; mostly decrease in beat rate. However, no concrete explanation can be given to the increase of beat rate in a group of cells but this is most likely associated to the types of cells present. Conversely, if fluid flow (e.g. blood) is to be considered, both decrease in either beat rate or beat strength can reduce the flow rate which is the common purpose for administering this drug.

Fig. 6e–6h shows the result of exposing a single cell (Movie 8) and a group of cells (Movie 10) with isoproterenol for 10

min (Movie 9 for single cell and Movie 11 for group of cells). Isoproterenol is known to increase the beat rate[30] and was formerly used in treating asthma. It is a β-adrenergic agonist and, therefore, affects the calcium ion channels and subsequently increases the beat rate. A single cell exposed to isoproterenol had 2x increase in beat rate, 1.5x increase in beat strength, and 20% decrease in beat duration. For a group of cell, 43% increase in beat rate, 5% decrease in beat strength, and 40% decrease in beat duration were observed.

Beat motion of the cells can depend on the concentration of the drugs administered. Using image-based analysis, the inotropism, lusitropis, chronotropism of the drugs can be profiled.[18,31] A common trend of drug effect was observed for all observed single cells exposed to the drugs. In contrary, varying results were observed for cells in a group which is associated to the different gating behavior of the gap junctions among the cells. Heteregoneity of the cells continues to be a problem in cardiomyocyte study. This requires further study and is beyond the scope of this report.

Conclusions

Centrifugal microfluidics was successfully utilized in studying single cardiomyocytes and a group of cells in the same prepared chip. Location of previously observed cells was made easy because of the predetermined trap sites which maximized the utility of image correlation analysis. Immunostaining, as one of the common technique in cell analysis, was successfully done in the chip. The result of β-actin immunostaining in single cell level validates the claim that a highly contracting cardiomyocyte has well organized cytoskeleton. More importantly, the applicability of the design chip as an *in vitro* cardiomyocyte-based drug screening and profiling platform was demonstrated. It is expected that these findings could aid in profiling the pharmacological effects of a drug and for future chip design and operation for high-throughput lab on-a-chip devices.

Notes and references

1 S. Whitebread, J. Hamon, D. Bojanic and L. Urban, *Drug Discov. Today*, 2005, **10**, 1421–1433.
2 V. Ahuja and S. Sharma, *J. Appl. Toxicol.*, 2014, **34**, 576–94.
3 I. Kola and J. Landis, *Nat. Rev. Drug Discov.*, 2004, **3**, 711–715.
4 M. Liu, Y. Wu, Y. Chen, J. Sun, Z. Zhao, X. -W. Chen, M. E. Matheny and H. Xu, *J. Am. Med. Informatics Assoc.*, 2012, **19**, e28–e35.
5 H. G. Laverty, C. Benson, E. J. Cartwright, M. J. Cross, C. Garland, T. Hammond, C. Holloway, N. McMahon, J. Milligan, B. K. Park, M. Pirmohamed, C. Pollard, J. Radford, N. Roome, P. Sager, S. Singh, T. Suter, W. Suter, a. Trafford, P. G. a Volders, R. Wallis, R. Weaver, M. York and J. P. Valentin, Br. *J. Pharmacol.*, 2011, **163**, 675–693.
6 B. Xi, N. Yu, X. Wang, X. Xu and Y. A. Abassi, *Biotechnol. J.*, 2008, **3**, 484–495.
7 T. Morijiri, M. Yamada, T. Hikida and M. Seki, *Microfluid. Nanofluidics*, 2013, **14**, 1049–1057.
8 J. Autebert, B. Coudert, F. C. Bidard, J. Y. Pierga, S. Descroix, L. Malaquin and J. L. Viovy, *Methods,* 2012, **57**, 297–307.
9 R. Burger and J. Ducrée, *Expert Rev. Mol. Diagn.*, 2012, **12**, 407–421.
10 R. Burger, D. Kirby, M. Glynn, C. Nwankire, M. O'Sullivan, J. Siegrist, D. Kinahan, G. Aguirre, G. Kijanka, R. a. Gorkin and J. Ducrée, *Curr. Opin. Chem. Biol.*, 2012, **16**, 409–414.
11 R. Gorkin, J.-M. J. Park, J. Siegrist, M. Amasia, B. S. Lee, J.-M. J. Park, J. Kim, H. Kim, M. Madou and Y.-K. Cho, *Lab Chip*, 2010, **10**, 1758–1773.
12 R. Burger, D. Kurzbuch, R. Gorkin, G. Kijanka, M. Glynn, C. McDonagh and J. Ducrée, *Lab Chip*, 2015, **15**, 378–381.
13 V. Lecault, A. K. White, A. Singhal and C. L. Hansen, *Curr. Opin. Chem. Biol.*, 2012, **16**, 381–390.
14 C. K. Byun, K. Abi-Samra, Y.-K. Cho and S. Takayama, *Electrophoresis*, 2013, **35**, 245–257.
15 R. Burger, P. Reith, G. Kijanka, V. Akujobi, P. Abgrall and J. Ducrée, *Lab Chip*, 2012, **12**, 1289.
16 R. Burger, P. Reith, V. Akujobi and J. Ducrée, *Microfluid. Nanofluidics*, 2012, **13**, 675–681.
17 D. Di Carlo, L. Y. Wu and L. P. Lee, *Lab Chip*, 2006, **6**, 1445–1449.
18 T. Hayakawa, T. Kunihiro, T. Ando, S. Kobayashi, E. Matsui, H. Yada, Y. Kanda, J. Kurokawa and T. Furukawa, *J. Mol. Cell. Cardiol.*, 2014, **77**, 178–191.
19 C. Bazan, D. Torres Barba, P. Blomgren and P. Paolini, *Int. J. Biomed. Imaging*, 2011, **2011**.
20 A. Kamgoué, J. Ohayon, Y. Usson, L. Riou and P. Tracqui, *Cytom. Part A*, 2009, **75**, 298–308.
21 J. Nilsson, M. Evander, B. Hammarström and T. Laurell, *Anal. Chim. Acta*, 2009, **649**, 141–157.
22 W. Espulgar, Y. Yamaguchi, W. Aoki, D. Mita, M. Saito, J.-K Lee and E. Tamiya, *Sensors Actuators B Chem.*, 2015, **207**, 43–50.
23 M. D. Bootman, I. Smyrnias, R. Thul, S. Coombes and H. L. Roderick, *Biochim. Biophys. Acta - Mol. Cell Res.*, 2011, **1813**, 922–934.
24 A. Skwarek-Maruszewska, P. Hotulainen, P. K. Mattila and P. Lappalainen, *J. Cell Sci.*, 2009, **122**, 2119–2126.
25 Y. Yaniv, M. D. Stern, E. G. Lakatta and V. A. Maltsev, *Biophys. J.*, 2013, **105**, 1551–1561.
26 Y. Yaniv, I. Ahmet, J. Liu, A. E. Lyashkov, T. R. Guiriba, Y Okamoto, B. D. Ziman and E. G. Lakatta, *Hear. Rhythm*, 2014, **11**, 1210–1219.
27 J. W. Smyth and R. M. Shaw, in *Methods in Enzymology*, Elsevier, 1st edn., 2012, **505**, 187–202.
28 J. S. Schulte, A. Scheffler, D. Rojas-Gomez, F. W. Mohr and S. Dhein, *Cell Commun. Adhes.*, 2008, **15**, 13–25.
29 A. Roy, W. C. Fields, C. Rocha-Resende, R. R. Resende, S. Guatimosim, V. F. Prado, R. Gros and M. A M. Prado, *FASEB J.*, 2013, **27**, 5072–5082.
30 E. J. Whalen and S. J. Lewis, *Eur. J. Pharmacol.*, 1999, **382**, 207–210.
31 M. M. Hossain, E. Shimizu, M. Saito, S. R. Rao, Y. Yamaguchi and E. Tamiya, *Analyst*, 2010, **135**, 1624–1630.

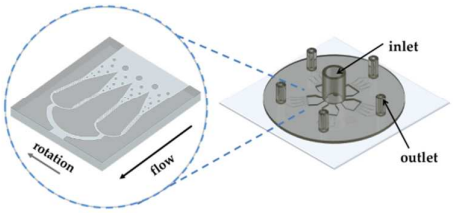

single-cell level drug profiling application of isolated single and group of neonatal rat cardiomyocytes trapped by centrifugal force.